The Activated Stroma Index Is a Novel and Independent Prognostic Marker in Pancreatic Ductal Adenocarcinoma

MERT ERKAN,* CHRISTOPH W. MICHALSKI,*,‡ SIMON RIEDER,* CAROLIN REISER–ERKAN,* IVANE ABIATARI,* ARMIN KOLB,‡ NATHALIA A. GIESE,‡ IRENE ESPOSITO,§ HELMUT FRIESS,* and JÖRG KLEEFF*

*Department of General Surgery, Technische Universität München, Munich, Germany; ‡Department of General Surgery, University of Heidelberg, Heidelberg, Germany; and the §Institute of Pathology, Technische Universität München, Munich, Germany

Background and Aims: **Pancreatic ductal adenocarcinoma (PDAC) is a highly desmoplastic tumor with an innate resistance to therapy. Pancreatic stellate cells (PSCs) produce this excessively desmoplastic microenvironment. The impact of PSC activity on PDAC behavior in vivo is analyzed.** ***Methods:*** **233 patients who underwent surgery for PDAC were evaluated by immunohistochemistry using antibodies against α-smooth muscle actin as a marker of PSC activity. Aniline was used to stain collagen deposition. The ratio of α-smooth muscle actin–stained area to collagen-stained area was defined as the activated stroma index (ASI). Survival analysis was performed using the Kaplan–Meier method. Prognostic factors were determined in a multivariable analysis using a Cox proportional hazards model.** ***Results:*** **Four major patterns of collagen deposition were defined with regard to PSC activity. The combination of high stromal activity and low collagen deposition was associated with a worse prognosis, whereas the combination of high collagen deposition and low stromal activity indicated a better prognosis. Patients with the lowest ASI had the best median survival rate (25.7 mo). The highest ASI was found in patients with the worst median survival rate (16.1 mo; $P = .007$; lowest vs highest ASI: hazard ratio, 1.61; 95% confidence interval, 1.014–2.562). ASI was an independent prognostic marker in multivariable survival analysis comparable with the nodal status of cancer.** ***Conclusions:*** **The activated stroma index is a novel independent prognostic marker in PDAC in cases undergoing surgery. This finding highlights the impact of the microenvironment in cancer progression and on patient survival.**

A unique property of pancreatic ductal adenocarcinoma (PDAC) is its excessive desmoplastic reaction, which is rarely observed in other tumors of the pancreas.[1,2] Pancreatic stellate cells (PSCs) have been identified as the main producers of this abundant extracellular matrix (ECM).[3] Once activated by cancer cells, PSCs may remain active via autonomous loops.[2,4]

Formerly, the peritumoral desmoplastic reaction was thought to have a protective function.[5] Recent evidence, however, suggests that the activated stroma can have promalignant attributes and may even initiate carcinogenesis.[6–8] In PDAC, several components of the ECM, including collagen-type1, have been shown to promote tumor growth, therapy resistance, and metastasis.[2,9]

Although the desmoplastic tissue in PDAC is a product of activated PSCs, the highest ECM deposition is not always found where the highest stromal activity is detected. In peritumoral areas, PSCs may outnumber the cancer cells without significant ECM deposition.[2,10] In contrast, vast amounts of desmoplastic tissue may contain only a few PSCs.[2] This variance may occur because pancreatic cancer cells can stimulate the PSCs located very close to them more than others that are not in their immediate vicinity.[2,4,10,11] With regard to the temporal sequence of events, α-smooth muscle actin (α-SMA) expression, which reflects PSC activity, should precede collagen deposition because it is the product of the activated PSCs. Through their production of matrix metalloproteinases, both PSCs and cancer cells can degrade the previously deposited ECM.[6,11–13] Thus, turnover of the ECM is a dynamic process, and immunohistochemical analysis of a specimen reveals areas with different disease duration and stromal activity.

Recently, it was reported that the activity of stromal myofibroblasts in colorectal cancer predicts disease recurrence.[8] We and others have shown previously that pancreatic cancer cells activate stellate cells, and that PSCs in turn promote tumor growth and chemoresistance through excessive ECM production in vitro.[2,4,11] In the current study, we quantified the amount of PSC activity and collagen deposition in resected specimens of PDAC patients and assessed their impact on clinicopathologic parameters. We also defined a novel marker for the activated stroma—the activated stroma index (ASI)—and proved its clinical relevance.

Materials and Methods

Clinical Data and Pancreatic Tissue Collection

Demographic, surgical, and pathologic data from a prospectively registered data base were analyzed retrospectively. Tissue collection and preservation were performed as described previously.[14] The use of human material for analysis was approved by the ethics committee of the University of Heidelberg in Germany. Written informed consent was obtained from all patients.

Abbreviations used in this paper: α-SMA, α smooth muscle actin; ASI, activated stroma index; ECM, extracellular matrix; PDAC, pancreatic ductal adenocarcinoma; PSC, pancreatic stellate cells.

1542-3565/08/$34.00
doi:10.1016/j.cgh.2008.05.006

Immunohistochemical Analysis and Computer-Assisted Image Analysis

Paraffin-embedded tissue blocks of 300 pathologically confirmed PDAC patients undergoing surgery between January 2002 and November 2006 at the Department of Surgery, University of Heidelberg, were evaluated. Sixty-seven blocks were excluded from the final analysis because of either low tissue quality (n = 11), predominance of peritumoral normal tissue rather than tissue from the cancerous area (n = 54), or incomplete clinical data (13 patients were lost to follow-up evaluation). Although the exclusion of the unsuitable blocks was made blinded to the clinical data, the possibility of an inadvertent selection bias was additionally excluded by comparing the demographic and clinicopathologic parameters of both cohorts. Immunohistochemical analyses of α-SMA and collagen in 233 samples were performed according to the manufacturer's instructions, as described previously.[2,14,15] Briefly, 2 consecutive 3-μm–thick sections were stained with an α-SMA antibody (1:1500, M0851; DAKO Cytomation, Hamburg, Germany) and with the collagen specific aniline blue of the Masson trichrome staining without applying hematoxylin or Biebrich scarlet-acid fuchsin as counterstaining. Slides were scanned with a Nikon coolscan V (Nikon Corp, Tokyo, Japan) at 4000 dots per inch. The digital images then were analyzed for the total surface area versus stained area using Adobe Photoshop 7.0 (Adobe Systems Inc, San Jose, CA). Briefly, an initial histogram was obtained to quantify the surface area in pixels. The

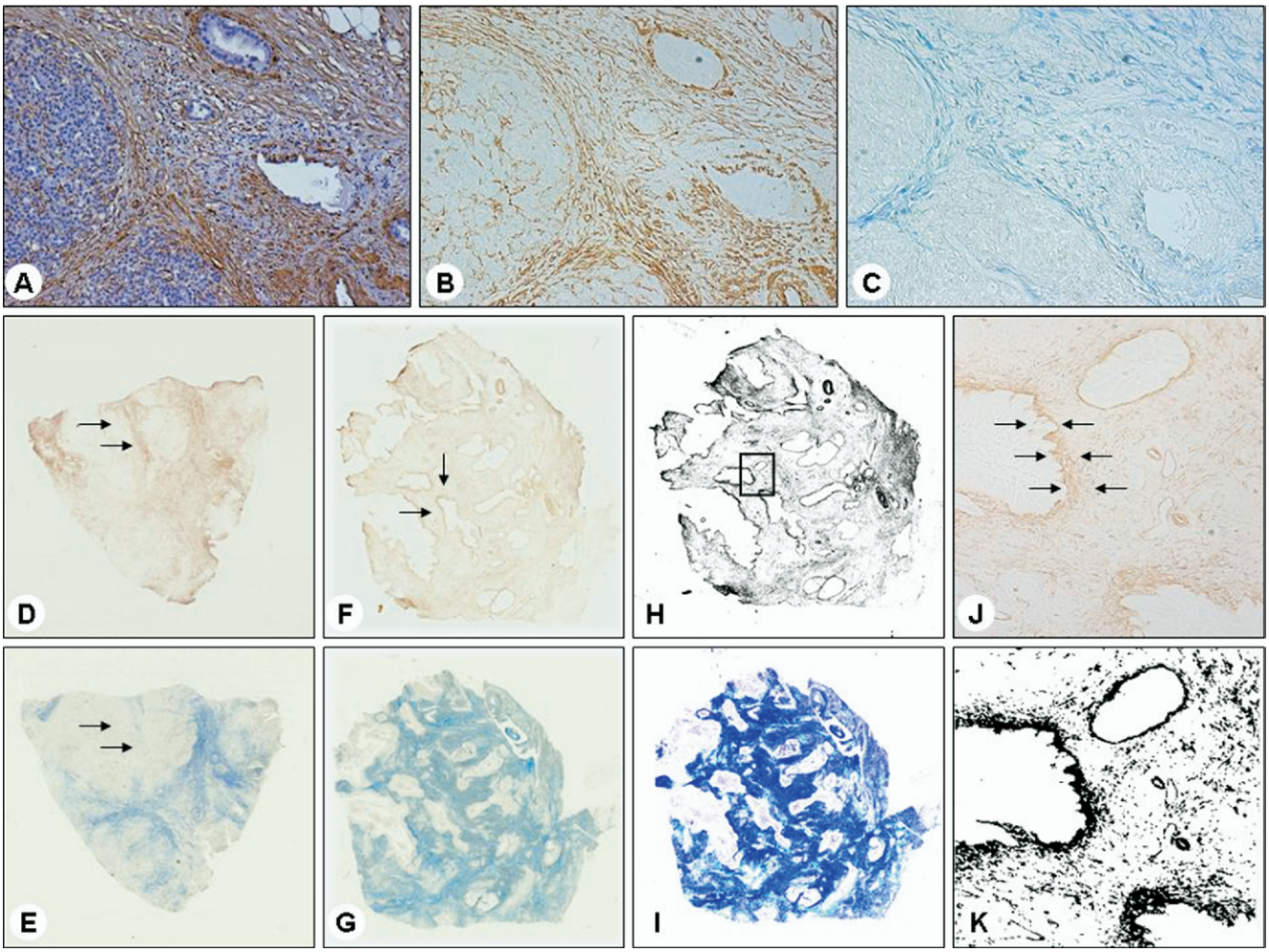

Figure 1. PSC patterns of activity with respect to collagen deposition and image analysis. α-SMA specifically stains the PSCs and vascular smooth muscle cells, whereas all other structures within the pancreas remain nonstained (*A* with hematoxylin counterstaining, *B* without counterstaining). (*C*) Aniline is a collagen-specific dye that does not stain any other structure (magnification, 100×). Scanned images of tissues; peritumoral chronic pancreatitis-like changes stained for (*D*) α-SMA and (*E*) aniline. (*D* and *E*) In periacinar spaces prominent α-SMA staining was visible where collagen had not yet been deposited (*arrows*). (*F* and *J*) Notice the increased density of α-SMA–expressing PSCs that are located in the immediate vicinity of cancer cells (*arrows*) and (*G*) stromal collagen deposition. Sections were scanned with the Nikon coolscan V at 4000 dots per inch. The digital images then were analyzed in single color for the total surface area (in pixels) versus the stained area using Adobe Photoshop 7.0. The upper and the lower input levels were overlapped to create black or white images (blue and white for aniline) without an intermediate zone. The ideal sensitivity of detection was achieved when the point of overlap corresponded to the vertex of the initial exponential phase of the histogram curve. Appearance of a section after image processing for (*H*) α-SMA and (*I*) collagen. Comparison of image quality: (*J*) Zeiss Axiocam 3.1 system coupled with the KS300 3.0 program at 50× magnification. (*K*) Magnified picture of the framed area in the scanned image (*H*).

histograms were analyzed in single color therefore, for the quantification of α-SMA–stained brown areas (red and blue), the image was converted to grey scale while aniline was analyzed in the blue channel. The upper and the lower input levels were overlapped to create black or white images (blue and white for aniline) without an intermediate zone. The ideal sensitivity of detection was achieved when the point of overlap corresponded to the vertex of the initial exponential phase of the histogram curve. After the optimal detection was identified, these values were kept constant throughout the analysis.

Color artifacts and major arteries were excluded manually from the analysis by the operator. This was performed on both slides by meticulously encircling staining artefacts or major arteries and deleting them from the image before measurement. The median surface area analyzed was 159 mm^2/section, which corresponds to more than 1000 high-power fields (200×). The immunohistochemical analysis and quantification of the ASI was made blinded to clinical data.

Assessment of Accuracy and Reproducibility of Color Analysis

To evaluate the accuracy and speed of this novel method of color analysis, the results of 10 sections were compared with results of automated color analysis using a Zeiss Axiocam 3.1 system coupled with the KS300 3.0 program at 200× magnification (Zeiss, Jena, Germany), as published previously.[8,16] The variance was less than 0.6%. The average time required for scanning and color assessment of a section with approximately 1 cm^2 surface area using a slide scanner and Adobe Photoshop was less than 3 minutes, compared with more than 1 hour for the method using the Zeiss Axiocam. Because the variable amount of nonstromal components (acini, islets, ducts, and cancer structures), which are stained neither by α-SMA nor by aniline, can change the ratio of collagen and α-SMA–stained area to the total surface area, we evaluated the consistency of our results within the same tumor. In 5 different patients, 5 random sections were made within each tumor.

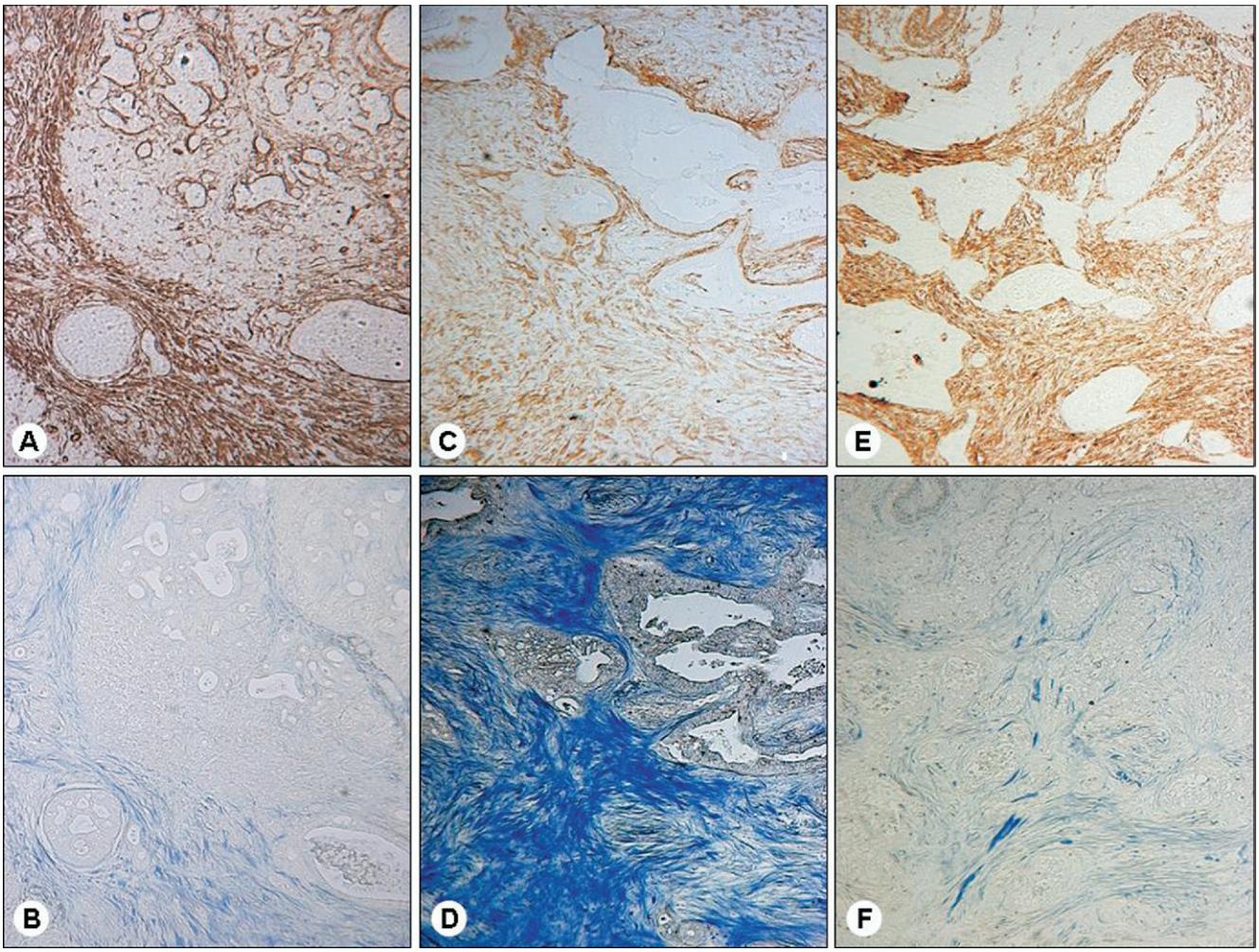

Figure 2. Patterns of stellate cell activity and collagen deposition around cancer structures. Immunohistochemistry analysis was performed using an anti–α-SMA antibody to detect activated PSCs and aniline to stain collagen fibers (magnification, 200×). (*A* and *C*) Within the cancerous area, the density of activated PSCs increased around cancer (unstained) structures. (*A* and *B*) Collagen deposition generally colocalized with the areas of activated PSCs. (*C* and *D*) In some sections there were fewer PSCs where prominent collagen deposition was seen. (*E* and *F*) In some other sections, although the PSC activity was intense, the collagen deposition was very low.

There was no statistically significant difference between the variations of α-SMA, collagen, and ASI.

Statistical Analysis

Statistical analyses were performed using SPSS 15.0 for Windows (SPSS Inc, Chicago, IL). Median values were taken as cut-off limits when 2 groups were compared. Survival analyses were performed using the Kaplan–Meier method for estimation of event rates and the log-rank test for survival comparisons between patient groups. Multivariable analysis was performed using a Cox proportional hazards model. Median survival and estimations of hazard ratios were reported with 95% confidence intervals. Comparison of demographic and clinicopathologic data between groups was made using the chi-square test. The distribution of ASI between discrete variables was assessed using the Mann–Whitney *U* test. Statistical significance was set at a *P* value of less than .05. SPSS 15.0 for Windows or GraphPad Prism 4 (GraphPad, San Diego, CA) software was used to present graphs.

Results

Peritumoral Activation of Pancreatic Stellate Cells and Deposition of Collagen

Four major patterns of collagen deposition were observed with regard to PSC activity (α-SMA expression). In chronic pancreatitis-like changes of the peritumoral stroma, interlobar septa were broadened where strong α-SMA staining colocalized with strong collagen staining (Figure 1*A*, *B*, *D*, and *E*). On the invasive front of the activated stroma, prominent α-SMA staining was visible in the periacinar spaces where collagen had not yet been deposited (Figure 1*D* and *E*, *arrows*). Within the cancerous area, the density of PSCs intensified around cancer structures (Figure 1*F* and *J*, *arrows*,

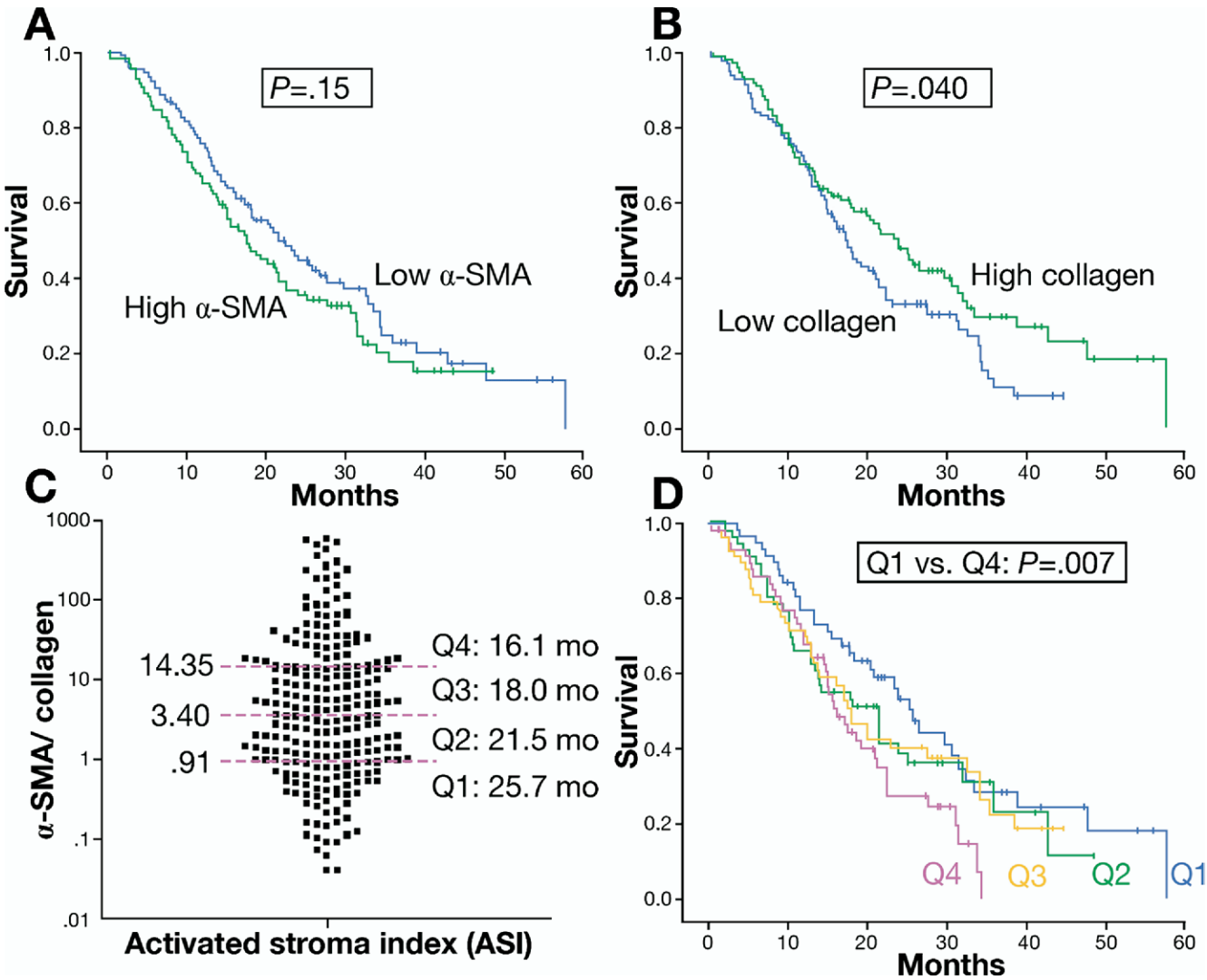

Figure 3. Correlation of collagen deposition, α-SMA expression, and ASI with survival of patients. Median values of the cohort for α-SMA and aniline staining were taken as cut-off limits to define groups with high (*green line*) and low (*blue line*) PSC activity as well as high (*green line*) and low (*blue line*) collagen deposition, respectively. The median survival of patients in these groups was compared with Kaplan-Meier analysis and the log-rank test. Survival analysis of patients with (*A*) high versus low PSC activity and (B) high versus low collagen deposition. The ratio of the α-SMA–stained area to the collagen-stained area was used to define the ASI. (*C*) Four quartiles with equal patient numbers were created using the cut-off values shown. (*D*) When the survival of patients in each quartile was compared, the survival of patients decreased as ASI increased.

Table 1. Patient Characteristics in the Whole Cohort and in ASI Quartiles

	n = 300	n = 233	χ^2	ASI Q1	ASI Q2	ASI Q3	ASI Q4	Mann-Whitney *U* test
Median age, y	65.1	65.3		61.7	63.7	66.1	67.0	$P = .11^a$
Sex			$P = .67$					$P = .98$
Female	45%	42%		47%	66%	60%	52%	
Male	55%	58%		53%	34%	40%	48%	
T status			$P = .76$					$P = .14$
T1 + T2	5%	6%		7%	9%	9%	2%	
T3 + T4	95%	94%		93%	91%	91%	98%	
N status			$P = .60$					$P = .50$
N0	19%	22%		31%	14%	22%	22%	
N1	81%	78%		69%	86%	78%	78%	
M status			$P = .35$					$P = .55$
M0	93%	96%		93%	95%	90%	91%	
M1	7%	4%		7%	5%	10%	9%	
Grade			$P = .76$					$P = .93$
G1	5%	6%		5%	3%	12%	3%	
G2 + G3	95%	94%		95%	97%	88%	97%	
Median actuarial survival, mo	20.4	20.3		25.7	21.5	18.0	16.1	
Resectability	100%	100%		100%	100%	100%	100%	

Q, ASI quartile; N1, metastasis to primary lymph nodes; M1, metastasis to interaortocaval lymph nodes.
[a]Age, younger than 65.3 years/older than 65.3 years.
χ^2 test was used to analyze the distribution of parameters in the whole cohort (n = 300) versus patients assessed (n = 233), whereas the Mann–Whitney *U* test was used to analyze the distribution of parameters in different ASI quartiles.

and Figure 2). In some sections there was prominent collagen deposition around the cancer structures without significant α-SMA expression (Figure 2*C* and *D*). In contrast, in some other sections, although the PSC activity was intense, the collagen deposition was very low (Figure 2*E* and *F*). In several sections, more than one pattern was observed in different areas.

High α-Smooth Muscle Actin–to-Collagen Ratio Is Correlated With a Worse Prognosis

Median values of the cohorts were taken as cut-off limits to compare patients with high/low stellate cell activity as well as high/low collagen deposition. High PSC activity indicated a tendency for a worsened prognosis (Figure 3*A*; $P = .15$). In contrast, high collagen deposition was correlated with significantly better survival in otherwise comparable patients (Figure 3*B*, Tables 1 and 2; $P = .040$).

Although the activated PSCs are the main producers of collagen, this paradoxic correlation with survival necessitated the use of an index comprising both parameters. We therefore defined the ASI as the area of α-SMA staining (active component of the stroma) divided by the area of collagen staining (quiescent component of the stroma) measured in consecutive sections. When the whole cohort was divided into 4 quartiles according to the ASI (Figure 3*C*), low stromal activity and high collagen deposition correlated with a better outcome (low ASI: median survival, 25.7 mo; 95% confidence interval, 21.8–29.6), whereas a high ASI indicating increased stromal activity but low collagen deposition correlated with poor survival (16.1 mo; 95%

Table 2. Patient Characteristics and Results of Univariable and Multivariable Analyses

	Median actuarial survival, mo	UVA	MVA	HR	95% confidence interval
Age, >65.3/<65.3 y	17.9/21.6	0.440	0.200	1.24	0.893–1.720
Sex, male/female	18.7/20.9	0.630	0.63	1.12	0.788–1.591
T3 + T4/T1 + T2	18.4/31.4	0.070	0.126	1.73	0.856–3.503
N1/N0	17.3/26.6	**0.030**	**0.040**	**1.54**	**1.020–2.337**
M1/M0	14.9/21.2	**0.010**	0.077	1.65	0.947–2.870
G2 + 3/G1	18.1/NR	**0.003**	**0.003**	**4.64**	**1.702–12.34**
COL L/H	17.5/23.9	**0.040**	**0.045**	**1.49**	**1.007–1.946**
SMA H/L	17.5/21.6	0.150	0.167	1.27	0.905–1.780
ASI H/L	17.2/23.4	0.073	**0.022**	**1.46**	**1.056–2.022**
Q4 *vs* Q1	16.1/25.7	**0.007**	**0.044**	**1.61**	**1.014–2.562**
All others *vs* Q1	17.9/25.7	0.051	**0.050**	**1.47**	**0.999–2.167**
Q4 *vs* all others	16.1/21.5	**0.030**	0.126	1.33	0.922–1.929

NOTE. Median values of the cohort were used to define the cut-off limits for age, collagen staining, α-SMA staining, and ASI.
Q, ASI quartile; UVA, univariable survival analysis, *P* value log-rank test; MVA, multivariable survival analysis, *P* value Cox ph-regression model; HR, hazard ratio of the MVA; COL H/L, collagen, high (H): > median, low (L): < than median value; SMA H/L, α-SMA, H: > median, L: < median value; N1, metastasis to primary lymph nodes; M1, metastasis to interaortocaval lymph nodes; G, grade of the tumor; NR, not reached.
Statiscally significant ($P < .05$) values are shown in bold characters.

confidence interval, 13.4–18.9). The median actuarial survival of patients in each quartile consistently decreased (25.7 vs 21.5 vs 18.0 vs 16.1 mo; Figure 3*C* and *D*) as the ASI increased, without a change in the distribution of sex, age, tumor size, nodal status (N), metastasis to the interaortocaval lymph nodes (M), and grade of the tumors (Figure 3, Table 1). The median difference in survival between quartile 1 (low stromal activity) and quartile 4 (high stromal activity) was 9.6 months (Figure 3*D*, Table 2; $P = .007$) in favor of the former.

Activated Stroma Index Is an Independent Prognostic Factor in Pancreatic Ductal Adenocarcinoma

To assess the dependence of ASI on other well-known prognostic markers, a multiple Cox regression analysis was performed. In one factor analysis, factors that correlated significantly with survival included nodal status (N), metastasis to interaortocaval lymph nodes (M), histologic grade of the tumor (G), ratio of stained area of collagen to total surface area, and ASI (Table 2). Being in quartile 1 was correlated with significantly better survival (25.7 vs 17.9 mo; $P = .050$) compared with the rest of the cohort, whereas being in quartile 4 was associated with shorter survival (16.1 vs 21.5 mo; $P = .126$). Multivariable analysis revealed that G1 versus G2/3, N0 versus N1, high versus low collagen deposition, and high versus low ASI were independent prognostic factors (Table 2).

Discussion

The most important finding of the current study is the identification of the activity of the stromal component in PDAC as an independent prognostic marker in surgical cases.

At the genetic level, pancreatic cancer is a well-characterized neoplasm. By contrast, the molecular mechanisms linking the genetic changes to the aggressive nature of this disease remain poorly understood.[17] One promising new development is the appreciation of the role of the cancer-associated stroma.[18] Current evidence supports the concept that cancer manipulates its stroma by co-opting their normal neighbors.[6,19] Accordingly, stromal cells may depart from normalcy, co-evolving with their malignant neighbors to sustain the growth of the latter.[2,4,6,12,20] Presumably, without the influence of cancer cells, normal PSCs, when activated, deposit ECM proteins with a time lag in which α-SMA expression precedes collagen deposition. Under physiologic conditions, this fibrogenic activity may serve to confine a noxious stimulus, as is the case in the healing phase of acute pancreatitis.[21–23] Accordingly, this type of PSC activity was seen mostly in peritumoral chronic pancreatitis-like changes. Therefore, deposition of a collagen-rich stroma around a cancer may represent a physiologic effort to confine the cancer. For example, in colorectal cancer metastasis to liver, the presence of a capsule around the metastasis is correlated with a better prognosis.[5] In line with this argument, we have identified the deposition of a collagen-rich stroma in PDAC as an independent favorable prognostic factor. Because cancer cells are known to activate PSCs, it is possible that a rapidly enlarging tumor elicits a stronger stromal reaction.[2,4,10] Nevertheless, there was no statistically significant correlation between either the grade or the size of the tumor and the ASI.

On the other hand, development of an abnormal stroma may precede and promote tumorigenesis.[24,25] Recently, Guerra et al[26] showed that mice harboring a conditional K-Ras mutation that was turned on after birth developed full-blown cancers only after induction of pancreatitis. Therefore, another possible explanation for our observations could be that in some patients a highly activated stroma creates a more permissive microenvironment for the cancer. For example, active PSCs are also potent sources of vascular endothelial growth factor production, and in liver metastasis, hepatic stellate cell activity precedes endothelial sprouting, hence neoangiogenesis.[27–29] In any case, our findings underline the importance of stromal activity for tumor behavior because this activity proves to be an independent prognostic marker in PDAC.

Although we and others previously have shown that cancer cells stimulate PSCs in vitro to secrete more collagen, it is likely that the deposition and turnover of collagen in vivo depends on a multifactorial balance between PSCs, cancer cells, and inflammatory cells, all of which produce significant amounts of matrix metalloproteinases.[2,4,11,30,31] Therefore, it would be an oversimplification to reduce the stromal component of a tumor mass only to stellate cell activity and to collagen deposition and to disregard the impact of inflammatory and endothelial cells. Nevertheless, ASI as a surrogate marker for both the active and the quiescent components of the stroma proves to be a robust parameter reflecting the impact of the microenvironment on cancer behavior.

The resection margin of PDAC is another important prognostic factor.[32] During the period of tissue collection of the current study, a prospectively conducted study by Esposito et al[33] at our institution showed that a meticulous pathologic analysis can alter the R1 resection rate significantly. Thus, the resection margin was not taken into assessment in the current study because the tissue was collected during both periods with reported R1 resection rates of 14% (2002–2004) and 76% (2005–2006).[33]

Finally, our novel method of computer-aided color analysis using a slide scanner and commercially available software not only simplifies the quantification of stained areas, but also reduces the costs and the time required without a significant loss of quality.

In conclusion, the ASI, which reflects the turnover of the stroma, is a novel independent prognostic marker in patients undergoing surgery for PDAC, highlighting the role of the microenvironment in cancer progression.

References

1. Cubilla AL, Fitzgerald PJ. Morphological lesions associated with human primary invasive nonendocrine pancreas cancer. Cancer Res 1976;36:2690–2698.
2. Erkan M, Kleeff J, Gorbachevski A, et al. Periostin creates a tumor-supportive microenvironment in the pancreas by sustaining fibrogenic stellate cell activity. Gastroenterology 2007;132:1447–1464.
3. Bachem MG, Schneider E, Gross H, et al. Identification, culture, and characterization of pancreatic stellate cells in rats and humans. Gastroenterology 1998;115:421–432.
4. Bachem MG, Schunemann M, Ramadani M, et al. Pancreatic carcinoma cells induce fibrosis by stimulating proliferation and matrix synthesis of stellate cells. Gastroenterology 2005;128:907–921.
5. Lunevicius R, Nakanishi H, Ito S, et al. Clinicopathological significance of fibrotic capsule formation around liver metastasis from colorectal cancer. J Cancer Res Clin Oncol 2001;127:193–199.

6. Bissell MJ, Radisky D. Putting tumours in context. Nat Rev Cancer 2001;1:46–54.
7. Camps JL, Chang SM, Hsu TC, et al. Fibroblast-mediated acceleration of human epithelial tumor growth in vivo. Proc Natl Acad Sci U S A 1990;87:75–79.
8. Tsujino T, Seshimo I, Yamamoto H, et al. Stromal myofibroblasts predict disease recurrence for colorectal cancer. Clin Cancer Res 2007;13:2082–2090.
9. Shintani Y, Hollingsworth MA, Wheelock MJ, et al. Collagen I promotes metastasis in pancreatic cancer by activating c-Jun NH(2)-terminal kinase 1 and up-regulating N-cadherin expression. Cancer Res 2006;66:11745–11753.
10. Yen TW, Aardal NP, Bronner MP, et al. Myofibroblasts are responsible for the desmoplastic reaction surrounding human pancreatic carcinomas. Surgery 2002;131:129–134.
11. He Y, Liu XD, Chen ZY, et al. Interaction between cancer cells and stromal fibroblasts is required for activation of the uPAR-uPA-MMP-2 cascade in pancreatic cancer metastasis. Clin Cancer Res 2007;13:3115–3124.
12. Schneiderhan W, Diaz F, Fundel M, et al. Pancreatic stellate cells are an important source of MMP-2 in human pancreatic cancer and accelerate tumor progression in a murine xenograft model and CAM assay. J Cell Sci 2007;120:512–519.
13. Shek FW, Benyon RC, Walker FM, et al. Expression of transforming growth factor-beta 1 by pancreatic stellate cells and its implications for matrix secretion and turnover in chronic pancreatitis. Am J Pathol 2002;160:1787–1798.
14. Erkan M, Kleeff J, Esposito I, et al. Loss of BNIP3 expression is a late event in pancreatic cancer contributing to chemoresistance and worsened prognosis. Oncogene 2005;24:4421–4432.
15. Michalski CW, Shi X, Reiser C, et al. Neurokinin-2 receptor levels correlate with intensity, frequency and duration of pain in chronic pancreatitis. Ann Surg 2007;246:786–793.
16. Hu WG, Li JW, Feng B, et al. Vascular endothelial growth factors C and D represent novel prognostic markers in colorectal carcinoma using quantitative image analysis. Eur Surg Res 2007;39:229–238.
17. Li D, Xie K, Wolff R, et al. Pancreatic cancer. Lancet 2004;363:1049–1057.
18. Kleeff J, Beckhove P, Esposito I, et al. Pancreatic cancer microenvironment. Int J Cancer 2007;121:699–705.
19. Kitano H. Cancer as a robust system: implications for anticancer therapy. Nat Rev Cancer 2004;4:227–235.
20. Kinzler KW, Vogelstein B. Landscaping the cancer terrain. Science 1998;280:1036–1037.
21. Lugea A, Nan L, French SW, et al. Pancreas recovery following cerulein-induced pancreatitis is impaired in plasminogen-deficient mice. Gastroenterology 2006;131:885–899.
22. Michalski CW, Laukert T, Sauliunaite D, et al. Cannabinoids ameliorate pain and reduce disease pathology in cerulein-induced acute pancreatitis. Gastroenterology 2007;132:1968–1978.
23. Neuschwander-Tetri BA, Bridle KR, Wells LD, et al. Repetitive acute pancreatic injury in the mouse induces procollagen alpha1(I) expression colocalized to pancreatic stellate cells. Lab Invest 2000;80:143–150.
24. Barcellos-Hoff MH, Ravani SA. Irradiated mammary gland stroma promotes the expression of tumorigenic potential by unirradiated epithelial cells. Cancer Res 2000;60:1254–1260.
25. Blavier L, Lazaryev A, Dorey F, et al. Matrix metalloproteinases play an active role in Wnt1-induced mammary tumorigenesis. Cancer Res 2006;66:2691–2699.
26. Guerra C, Schuhmacher AJ, Canamero M, et al. Chronic pancreatitis is essential for induction of pancreatic ductal adenocarcinoma by K-Ras oncogenes in adult mice. Cancer Cell 2007;11:291–302.
27. Kordes C, Sawitza I, Muller-Marbach A, et al. CD133+ hepatic stellate cells are progenitor cells. Biochem Biophys Res Commun 2007;352:410–417.
28. Olaso E, Salado C, Egilegor E, et al. Proangiogenic role of tumor-activated hepatic stellate cells in experimental melanoma metastasis. Hepatology 2003;37:674–685.
29. Zhang W, Erkan M, Abiatari I, et al. Expression of extracellular matrix metalloproteinase inducer (EMMPRIN/CD147) in pancreatic neoplasm and pancreatic stellate cells. Cancer Biol Ther 2007;6:218–227.
30. Farrow B, Sugiyama Y, Chen A, et al. Inflammatory mechanisms contributing to pancreatic cancer development. Ann Surg 2004;239:766–771.
31. Michalski CW, Gorbachevski A, Erkan M, et al. Mononuclear cells modulate the activity of pancreatic stellate cells which in turn promote fibrosis and inflammation in chronic pancreatitis. J Transl Med 2007;5:63.
32. Neoptolemos JP, Stocken DD, Dunn JA, et al. Influence of resection margins on survival for patients with pancreatic cancer treated by adjuvant chemoradiation and/or chemotherapy in the ESPAC-1 randomized controlled trial. Ann Surg 2001;234:758–768.
33. Esposito I, Kleeff J, Bergmann F, et al. Most pancreatic cancer resections are R1 resections. Ann Surg Oncol 2008;15:1651–1660.

Address requests for reprints to: Jörg Kleeff, MD, Department of General Surgery, Technische Universität München, Klinikum rechts der Isar, 81675 Munich, Germany. e-mail: kleeff@gmx.de; fax: (49) 089-4140-4870.

Supported in part by a Postdoctoral Research Program grant from the University of Heidelberg (C.W.M.). This work has been supported by EU Framework Programme 6, Integrated Project—Mol Diag-Pa Ca (Molecular Diagnosis of Pancreatic Cancer).

The authors thank Ms Bruni Bentzinger, Mrs Magdalena Geiss, and Ms. Vesna Vukovic for excellent technical support. The authors are indebted to M.Sc. Tibor Schuster from the Institute of Medical Statistics and Epidemiology at the Technische Universität Munich, who helped with the statistical analyses.

M.E., C.W.M., and S.R. contributed equally to this article.